Proceedings of the
American Control Conference
Seattle, Washington • June 1995

Air to Fuel Ratio Control of Spark Ignition Engines Using Dynamic Sliding Mode Control and Gaussian Neural Network

Mooncheol Won*, Sei-Bum Choi †, and J.K. Hedrick‡
Department of Mechanical Engineering
University of California at Berkeley
Berkeley, CA94720

Abstract

This paper deals air to fuel ratio control of a spark ignition engine, whose pollutant is a major cause of air pollution. A direct adaptive control using Gaussian neural networks is developed to compensate transient fueling dynamics and measurement error in mass air flow rate into the cylinder. The transient fueling compensation method is coupled with a dynamic sliding mode control technique that governs the steady state fueling rate. The proposed controller is simple enough for on-line computation and is implemented on an automotive engine using a PC-386.

1 Introduction

The purpose of fuel injection control is to regulate the air to fuel (A/F) ratio at a desired ratio depending on the type of operations. These include warming up, power generation (rapid acceleration), constant high speed operation, and urban traffic mode. Among them, urban traffic mode is the largest contributor of air pollutants. The purpose of a catalytic converter is to oxidize excess levels of the tail pipe pollutants such as CO, HC, and NO_x. Unfortunately, the efficiency of the catalytic converter is high enough only in a very narrow range (around 14.7) of the A/F ratio [6].

The A/F ratio regulation is a very difficult control problem since the oxygen sensor at the exhaust gives only almost binary information (leanness or richness of the A/F ratio), and has considerable sensing time delay.

Many of the current production fuel-injection controllers rely on open-loop feed-forward control based on a look-up table with PI (proportional plus integral) feedback control. However, building this table is a laborious process of calibration and tuning.

As a solution to this problem, a sliding mode fuel-injection control method was proposed [3], [4]. This analytic design method is in good agreement with the binary nature of the oxygen sensor signal. However, the method has the problem of large amplitude chattering which is due to unavoidable oxygen sensor time-delay. The chattering problem limits the magnitude of the feedback gain. Yet, an appropriate amount of gain is required to guarantee the surface attraction condition under the existence of modeling errors. Both the "speed-density" method and the "mass-air-flow-meter" method have sufficient errors which force the gain to be increased. A dynamic sliding mode control method was suggested which considerably reduces the chattering [5]. This method is used in the steady state A/F ratio control in this paper.

There has been a great deal of research on transient air/fuel characteristics, and it is concluded that three characteristic delays are responsible for unwanted air/fuel ratio excursions during the transient operations [1], [7], [8]. These are the time-delay of the computer control system, a physical delay in the intake manifold, and a physical delay of the fuel flow which results from the finite rate of evaporation of the fuel film on the intake manifold and port walls. Matthews *et al.* suggested an intake and ECM (Engine Control Module) submodel and examined tip-in/tip-out behavior [8]. Hendricks *et al.* suggested a mean value engine model and an observer for A/F ratio control [7]. Chang *et al.* suggested a similar event-based observation control technique [2].

In this paper, a new transient fueling compensation technique is developed. The technique utilizes a direct adaptive sliding control method with Gaussian neural networks [9]. The transient fueling dynamics is identified on-line as a function of the rate of the throttle change and the mass air flow rate into the manifold. The advantage of this method is its robustness to engine aging and individual engine characteristics by using on-line adaptation.

The measurement error in the mass air flow rate into the cylinder is also compensated using the same technique. A one dimensional table is adapted on-line when throttle angle changes mildly.

This paper is organized as follows. In section 2, a fuel injection model for control is presented. Section 3 presents a dynamic sliding mode control method which governs steady state fueling rate. In section 4, a measurement error of mass air flow rate into manifold is compensated. In section 5, a method for compensating transient fuel delivery dynamics is developed. Section 6 presents numerical simulation and experimental results.

2 Fuel Injection Model

A schematic diagram of fuel injection problem is shown in Figure 1. The control problem is to vary the fuel-spray rate,

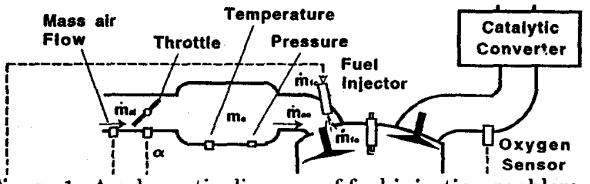

Figure 1: A schematic diagram of fuel injection problem

*PostDoc.
†PostDoc.
‡Professor

$\dot{m}_{fo}$, so that the air/fuel ratio remains close to stoichiometry even during the rapid throttle transient.

A simplified dynamic model [3], [5] for this problem is

$$\dot{m}_a = \dot{m}_{ai}(\alpha, m_a) - \dot{m}_{ao}(\omega_e, m_a) \quad (1)$$

$$\tau_f \ddot{m}_{fo}(t) = -\dot{m}_{fo}(t) + \dot{m}_{fc}(t - \Delta t_f) \quad (2)$$

The first equation is the air flow dynamics through the intake manifold. m_a is the mass of air in the intake manifold, ω_e is the engine speed, $\dot{m}_{ai}$ is the air-mass-flow rate into the manifold, and $\dot{m}_{ao}$ is the air-mass-flow rate out of the manifold which is given as a function of ω_e and m_a. The mass air flow rate into the manifold ($\dot{m}_{ai}$) is measured by a hot-wire sensor. The mass air flow rate out of the manifold ($\dot{m}_{ao}$) cannot be measured; but during steady state operations, is identical to $\dot{m}_{ai}$. Therefore, the steady state map of $\dot{m}_{ao}$ (Figure 2) can be obtained as a function of engine speed and manifold pressure by steady state engine tests. By denoting the

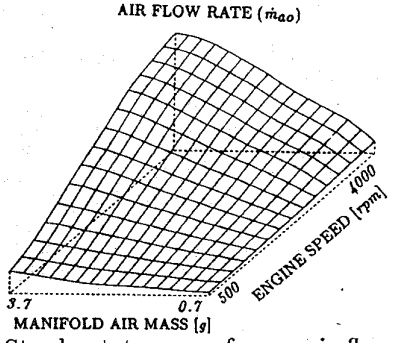

Figure 2: Steady state map of mass air flow rate into cylinder $\dot{m}_{ao}$

steady state air flow rate out of the manifold as $\dot{m}_{ao}(m_a, \omega_e)$, the true air flow rate during transient operations can be expressed as :

$$\dot{m}_{ao} = (1 + e)\, \dot{m}_{ao}(m_a, \omega_e) \quad (3)$$

where e is a multiplicative error fraction. For S.I. engines, the slope of the $\dot{m}_{ao}(m_a, \omega_e)$ map in the direction of m_a, is always positive. This characteristic is exploited in the dynamic sliding mode controller design.

The second equation is a linear approximation of fuel delivery dynamics. $\dot{m}_{fc}$ is the commanded fuel-injection spray rate, $\dot{m}_{fo}$ is the actual spray rate into the cylinder, τ_f is the fueling time constant, and Δt_f is the pure time delay. The pure time delay is caused by computation time delay and delays in opening the intake valves. The lag is due to the fuel wetting/evaporation on the intake wall. The $\tau - X$ fueling model [7] is well known, but does not include the pure time delay. It should be noted that X of a port fuel-injection system in the $\tau - X$ moel is a small quantity.

3 Dynamic Sliding Mode Control

Sliding mode control methods have been developed as a systematic way to design a controller for a nonlinear plant [10], [11]. Moreover, the binary nature of the measurement signal in fuel injection control is in good agreement with that of sliding mode control methods. The production oxygen sensor at the exhaust tells only the richness or leanness of the air to fuel mixture. The sensor also has a considerable time delay (t_d) which can be approximated by

$$t_d = 0.02 + \frac{4\pi}{\omega_e} \quad \text{(sec.)} \quad (4)$$

where ω_e is the engine speed in rad/sec. This considerable sensor delay induces large chattering of A/F ratio in both PI control and conventional sliding control methods [3]. Dynamic sliding mode control [5] reduces the chattering considerably, and decides the desired steady state fueling rate.

The objective of the fuel injection control is to maintain the air to fuel ratio close to 14.7(stoichiometry ratio). Since the initial conditions are reset to near zero after the exhaust stroke, an equivalent objective is to keep :

$$\frac{\dot{m}_{ao}}{\dot{m}_{fo}} = 14.7 = \beta \quad (5)$$

Deciding the rate of fuel to be injected is not trivial because the mass air flow rate into the cylinder, $\dot{m}_{ao}$, can not be measured. In this section, the desired $\dot{m}_{fo}$ will be calculated, and the compensation of fuel delivery dynamics is dealt in section 6 using Gaussian neural networks. A sliding surface is defined as :

$$s = \dot{m}_{ao} - \beta \dot{m}_{fo} \quad (6)$$

Then the control objective is to maintain s close to zero. The measurement output from the oxygen sensor, y, is expressed as :

$$y(t) = sign(s(t - t_d)) \quad (7)$$

The sliding surface is rewritten as :

$$s = (1 + e)\dot{\dot{m}}_{ao} - \beta \dot{m}_{fo} \quad (8)$$

Differentiation of the sliding surface yields :

$$\begin{aligned} \dot{s} &= \dddot{m}_{ao} + e\ddot{\dot{m}}_{ao} + \dot{e}\ddot{\dot{m}}_{ao} - \beta \ddot{m}_{fo} \\ &= \frac{\partial \ddot{\dot{m}}_{ao}}{\partial m_a} \dot{m}_a + \frac{\partial \ddot{\dot{m}}_{ao}}{\partial \omega_e} \dot{\omega}_e + e\ddot{\dot{m}}_{ao} + \dot{e}\ddot{\dot{m}}_{ao} - \beta \ddot{m}_{fo} \end{aligned}$$

Putting the manifold dynamics equation (1), and setting,

$$\beta \ddot{m}_{fo} = -\beta \frac{\partial \ddot{\dot{m}}_{ao}}{\partial m_a} \dot{m}_{fo} + \left(\frac{\partial \ddot{\dot{m}}_{ao}}{\partial m_a} \dot{m}_{ai} + \frac{\partial \ddot{\dot{m}}_{ao}}{\partial \omega_e} \dot{\omega}_e\right) + l\, y \quad (9)$$

the closed loop dynamics of the sliding surface becomes

$$\dot{s} = -\frac{\partial \ddot{\dot{m}}_{ao}}{\partial m_a} s + e\ddot{\dot{m}}_{ao} + \dot{e}\ddot{\dot{m}}_{ao} - l\, y \quad (10)$$

where l is a positive feedback gain. Since the slope $\partial \ddot{\dot{m}}_{ao} / \partial m_a$ is always positive (lies in between 15 and 20), the resulting closed loop dynamics is much faster than that of sliding mode control, which is given as [3]

$$\dot{s} = e\ddot{\dot{m}}_{ao} + \dot{e}\ddot{\dot{m}}_{ao} - l\, y \quad (11)$$

It can be shown that the chattering magnitude of A/F ratio in dynamic sliding mode control is only 20 % of that of sliding mode control [5].

The control, $\dot{m}_{fo}$, is obtained from the integration of (9), thus the term "dynamic" controller.

$$\begin{aligned} \dot{m}_{fo}(t) &= \dot{m}_{fo}(0) \\ &+ \frac{1}{\beta} \int_0^t \left[\frac{\partial \ddot{\dot{m}}_{ao}}{\partial m_a} (\dot{m}_{ai} - \beta \dot{m}_{fc}(\tau)) + \frac{\partial \ddot{\dot{m}}_{ao}}{\partial \omega_e} \dot{\omega}_e\right] d\tau \\ &+ \frac{1}{\beta} \int_0^t l\, y(\tau)\, d\tau \end{aligned}$$

This control law represents a good way to combine the speed-density method and the mass-air-flow-meter method.

4 Measurement Error Compensation in Mass Air Flow Rate into Manifold

Dynamic sliding mode control is very sensitive to the measurement error in the mass air flow rate into the manifold ($\dot{m}_{ai}$) since the closed loop dynamics is very fast, and the term containing $\dot{m}_{ai}$ acts as a forcing term in the closed loop dynamics. $\dot{m}_{ai}$ is measured by a hot wire sensor, and there is a nonlinear one-dimensional table that converts voltage measurement to mass air flow rate. Since the characteristics of the hot wire sensor can change with time (which is a main error source), the conversion table needs to be innovated. In this section, the measured $\dot{m}_{ai}$ is corrected from a one-dimensional function of itself. The function is identified on-line by a direct adaptive control method [9] using a Gaussian network.

By defining the measured mass air flow rate into the manifold as $\dot{m}_{aim}$, the corrected value of the mass air flow rate ($\dot{m}_{ai}$) is constructed using Gaussian functions:

$$\dot{m}_{ai} = \dot{m}_{aim}\left[1 + \sum_{i=1}^{m} \hat{d}_i exp\left(-\frac{r_i^2}{\sigma^2}\right)\right] \tag{12}$$

where r_i are the distance from a node on a $\dot{m}_{aim}$ axis (see Figure 3), σ is a constant, and $\hat{d}_i$ are the estimates of true parameters d_i. The true $\dot{m}_{ai}$ can be expressed as

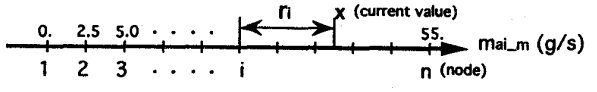

Figure 3: Neural network mesh of mass air flow rate into cylinder

$$\dot{m}_{ai} = \dot{m}_{aim}\left[1 + \sum_{i=1}^{m} d_i\ exp\left(-\frac{r_i^2}{\sigma^2}\right) + e_m\right] \tag{13}$$

where e_m is % error in the approximation.

Choose the sliding surface (s) and a Lyapunov function (V) as

$$s = \dot{m}_{ao} - \beta \dot{m}_{fo} \tag{14}$$

$$V = |s| + \frac{1}{\rho}\sum_{i=1}^{m} \tilde{d}_i^2 \tag{15}$$

where ρ is a positive constant and $\tilde{d}_i = d_i - \hat{d}_i$. Differentiation of V becomes

$$\dot{V} = \dot{s}sgn(s) + \frac{1}{\rho}\sum_{i=1}^{m} \dot{\tilde{d}}_i \tilde{d}_i \tag{16}$$

Under the control given as

$$\beta\ddot{m}_{fo} = -\beta\frac{\partial \dot{m}_{ao}}{\partial m_a}\dot{m}_{fo} + (\frac{\partial \dot{m}_{ao}}{\partial m_a}\ddot{m}_{ai} + \frac{\partial \dot{m}_{ao}}{\partial \omega_e}\ddot{\omega}_e) + lsgn(s) \tag{17}$$

(which is the same as the dynamic sliding control (9) except for the $\frac{\partial \dot{m}_{ao}}{\partial m_a}\ddot{m}_{ai}$ term), $\dot{s}$ becomes

$$\dot{s} = -\frac{\partial \dot{m}_{ao}}{\partial m_a}s + e\ddot{m}_{ao} + \dot{e}\dot{m}_{ao} + \frac{\partial \dot{m}_{ao}}{\partial m_a}\ddot{m}_{ai} - lsgn(s) \tag{18}$$

The estimation error in m_{ai} is expressed as:

$$\ddot{m}_{ai} = \dot{m}_{ai} - \dot{\hat{m}}_{ai} = \left[\dot{m}_{aim}\sum_{i=1}^{m} \tilde{d}_i exp\left(-\frac{r_i^2}{\sigma^2}\right)\right] + \dot{m}_{aim}\ e_m \tag{19}$$

Putting (18) into (16) yields

$$\begin{aligned}\dot{V} &= -\frac{\partial \dot{m}_{ao}}{\partial m_a}|s| + sgn(s)(e\ddot{m}_{ao} + \dot{e}\dot{m}_{ao} + \frac{\partial \dot{m}_{ao}}{\partial m_a}\dot{m}_{aim}e_m) \\ &\quad -l + \sum_{i=1}^{m} \dot{\tilde{d}}_i\left[sgn(s)\frac{\partial \dot{m}_{ao}}{\partial m_a}\dot{m}_{aim}exp\left(-\frac{r_i^2}{\sigma^2}\right) - \frac{1}{\rho}\dot{\hat{d}}_i\right]\end{aligned}$$

Choosing the adaptation law as

$$\dot{\hat{d}}_i = \rho\ sgn(s)\frac{\partial \dot{m}_{ao}}{\partial m_a}\dot{m}_{aim}exp\left(-\frac{r_i^2}{\sigma^2}\right) \tag{20}$$

yields

$$\dot{V} = -\frac{\partial \dot{m}_{ao}}{\partial m_a}|s| + sgn(s)(e\ddot{m}_{ao} + \dot{e}\dot{m}_{ao} + \frac{\partial \dot{m}_{ao}}{\partial m_a}\dot{m}_{aim}e_m) - l \tag{21}$$

Therefore for a large enough l, $\dot{V} < 0$ is guaranteed. The adaptation in the implementation is delayed by t_d since the $sgn(s(t))$ is available at time $t + t_d$. Also, the adaptation is activated only when the throttle changes slowly.

5 Transient Fuel Compensation

As will be seen in the experimental section, the dynamic compensator shows good performance during steady states (when the throttle angle change is not rapid). There are still undesirable peaks at both toe-in and toe-out. This is because there exist fuel delivery dynamics between the fueling commmand and the actual fueling into the cylinder. Here, it is assumed that

$$\dot{m}_{fo} = \dot{m}_{fc} - \dot{m}_{fot} \tag{22}$$

where $\dot{m}_{fot}$ is lost/added fueling rate due to the fuel delivery dynamics (see Figure 1).

In this section, the fuel flow rate command is corrected to compensate the unknown fuel delivery dynamics. Since the transient fuel delivery dynamics includes pure time delay, it is necessary to employ a feedforward controller using the engine variables that are faster than the mass air flow rate into the cylinder ($\dot{m}_{ao}$). The positive or negative amount of the transient fueling rate ($\dot{m}_{fot}$) is considered as a function of the rate of throttle change ($\dot{\alpha}$) and the mass air flow rate into the manifold ($\dot{m}_{ai}$). The total fuel command to the injector ($\dot{m}_{fc}$) is assumed as:

$$\dot{m}_{fc} = \dot{m}_{fos} + \dot{m}_{fot}(\dot{\alpha}, \dot{m}_{ai}) \tag{23}$$

where $\dot{m}_{fos}$ is the steady state fueling rate of the previous section, which is obtained by integrating equation (17) and $\dot{m}_{fot}$ is our estimate of the additional fuel rate required to compensate for the transient condition. The reason for choosing $\dot{\alpha}$ as an independent variable is that the rate of throttle change is faster than the mass air flow rate out of the manifold ($\dot{m}_{ao}$), and it decides the sign of the transient fueling rate ($\dot{m}_{fot}$). The mass air flow rate into the manifold ($\dot{m}_{ai}$) is selected because $\dot{m}_{ai}$ is faster than $\dot{m}_{ao}$, and is similar to ($\dot{m}_{fos}$). Putting (23) into (22) yields

$$\dot{m}_{fo} = m_{fos} + \dot{\hat{m}}_{fot} \tag{24}$$

where $\dot{\hat{m}}_{fot} = \dot{\hat{m}}_{fot} - \dot{m}_{fot}$. Therefore $\dot{\hat{m}}_{fot}$ is needed to be close to $\dot{m}_{fot}$. Sliding surface s is defined as

$$s = \dot{m}_{ao} - \beta \dot{m}_{fo} \tag{25}$$

Equivalently the sliding surface can be expressed as

$$s = \dot{m}_{ao} - \beta(\dot{m}_{fos} + (\dot{\hat{m}}_{fot} - \dot{m}_{fot})) \tag{26}$$

It is assumed that

$$\dot{\hat{m}}_{fot} = \sum_{i=1}^{m} \hat{c}_i \, exp\left(-\frac{r_i^2}{\sigma^2}\right) \tag{27}$$

where r_i is the Euclidian distance from a node on a $\dot{\alpha}$-$\dot{m}_{ai}$ grid (see Figure 4), and σ is a constant. $\hat{c}_i$ are our updated estimates of the "true" constant values. $\dot{\hat{m}}_{fot}$ can be expressed as:

$$\dot{\hat{m}}_{fot} = \sum_{i=1}^{m} c_i exp\left(-\frac{r_i^2}{\sigma^2}\right) + e_t \tag{28}$$

where e_t is an approximation error. A Lyapunov function is

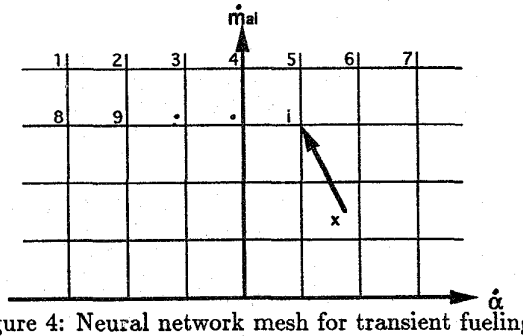

Figure 4: Neural network mesh for transient fueling

chosen as

$$V = |s| + \frac{1}{2g} \sum_{i=1}^{m} \tilde{c}_i^2 \tag{29}$$

where g is a positive constant. The absolute function is used because only the sign of s is available. Differentiation of V becomes

$$\dot{V} = \dot{s} sgn(s) + \frac{1}{g} \sum_{i=1}^{m} \tilde{c}_i \dot{\tilde{c}}_i \tag{30}$$

where $\tilde{c}_i = \hat{c}_i - c_i$. Using equations (17), (27) and (28) yields the expression for $\dot{s}$

$$\begin{aligned} \dot{s} &= -\frac{\partial \dot{m}_{ao}}{\partial m_a} s - \beta \frac{\partial \dot{m}_{ao}}{\partial m_a} \dot{\tilde{m}}_{fot} + e_2 - l sgn(s) \\ &\quad -\beta \sum_{i=1}^{m} \tilde{c}_i exp\left(-\frac{r_i^2}{\sigma^2}\right) \end{aligned} \tag{31}$$

where $e_2 = e\ddot{\hat{m}}_{ao} + \dot{e}\dot{\hat{m}}_{ao} + \frac{\partial \dot{m}_{ao}}{\partial m_a} \dot{\hat{m}}_{ai} + \beta \dot{e}_t$. Using equation (31) and $\dot{\tilde{c}}_i = \dot{\hat{c}}_i$, $\dot{V}$ becomes

$$\begin{aligned} \dot{V} &= -\frac{\partial \dot{m}_{ao}}{\partial m_a} |s| - l + e_2 sgn(s) \\ &\quad - \sum_{i=1}^{m} \tilde{c}_i \left[\beta exp\left(-\frac{r_i^2}{\sigma^2}\right) sgn(s) - \frac{1}{g} \dot{\hat{c}}_i\right] \end{aligned} \tag{32}$$

Choosing the adaptation laws for the coefficients c_i as

$$\dot{\hat{c}}_i = sign(s) \cdot g \cdot exp\left(-\frac{r_i^2}{\sigma^2}\right) \tag{33}$$

yields

$$\dot{V} = -\frac{\partial \dot{m}_{ao}}{\partial m_a} |s| - l + e_2 sgn(s) \tag{34}$$

where $\frac{\partial \dot{m}_{ao}}{\partial m_a} > 0$. Thus for a large enough l, $\dot{V} < 0$ is achieved. Our transient control $\dot{\hat{m}}_{fot}$ is given by integrating (27). Since at time t only $sign(s(t - t_d))$ is available from the oxygen sensor, the adaptation is delayed by t_d in actual implementation. Also, the adaptation or innovation of the table is activated only when the throttle change is larger than a threshold value.

6 Experimental results

The suggested controller was evaluated at the University of California Berkeley engine dynamometer test rig, and compared with a production ECM and a sliding mode controller. The engine used for the test is a 3.8 liter V-6 sequential port-injection S.I. engine. The air-mass-flow rate through the throttle body, the manifold air mass, pressure and temperature and the oxygen in the exhaust gas were measured using typical production engine sensors. A linear oxygen sensor (NISSAN model PLR-1) installed in the exhaust pipe was used only to monitor the A/F ratio.

In this study, all the experimental results are obtained under severe and realistic conditions: the dynamometer load is fixed; dynamometer inertia is the only external inertia; and the throttle varies in a small throttle opening zone where the manifold pressure changes rapidly. The throttle variation in the experiment is shown in Figure 5. With the external load fixed to 67.7 N-m, the variation induces large variation of the manifold pressure. During transient operation, the air to fuel ratio (Figure 6) of the developed control methods (dynamic sliding sliding mode control and direct adaptive control) give about 30 % smaller standard deviations than that of the production ECM (Figure 7). Comparing the duration times of the air to fuel ratio outside the 14.5 - 14.7 band, the proposed controller has less duration time than the production ECM. Figure 8 shows the compensated transient fueling rate. Sufficient learning process (on line adaptation of the constants, $\hat{c}_i$) has been preceded before obtaining the transient fueling rate map, $\dot{m}_{fot}(\dot{\alpha}, \dot{m}_{ai})$. Large peaks of the air to ratio are observed when the transient fuel compensation is not accompanied by dynamic sliding mode control (Figure 9) It is also seen that A/F ratio has significant drift from stoichiometry without the compensation of the measurement error in $\dot{m}_{ai}$ (Figure 10).

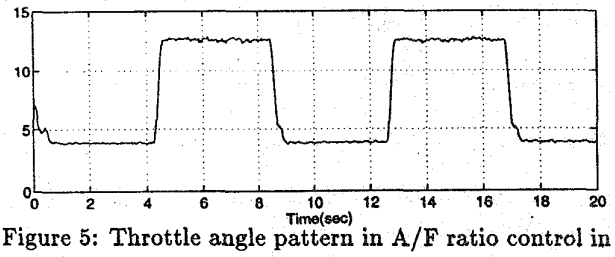

Figure 5: Throttle angle pattern in A/F ratio control in experiments

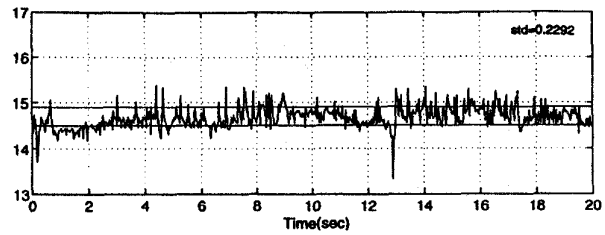

Figure 6: Air to fuel ratio of proposed control (direct adaptive control with dynamic sliding control)

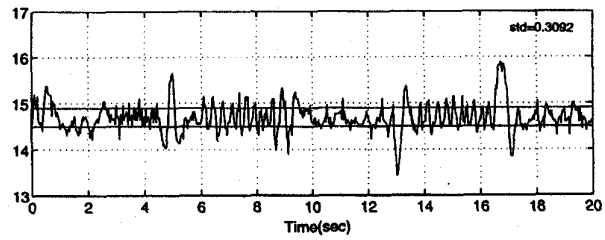

Figure 7: Air to fuel ration of production ECM

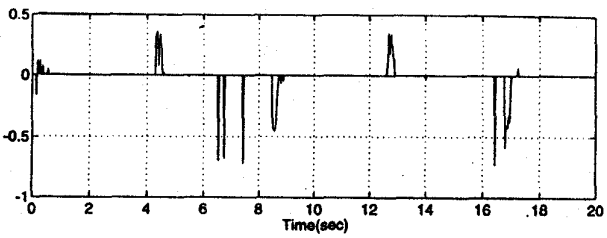

Figure 8: Compensated transient fueling rate

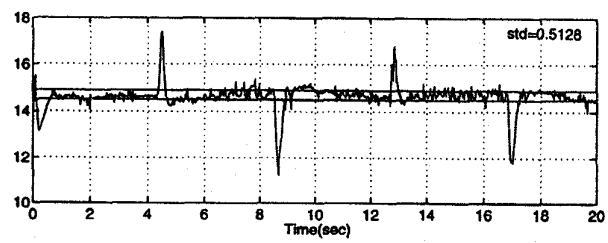

Figure 9: A/F ratio of dynamic sliding control without transient fuel compensation

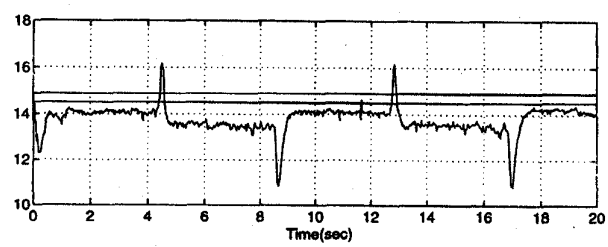

Figure 10: A/F ratio of dynamic sliding control without compensation of measurement error in $\dot{m}_{ai}$

7 Conclusion

The air to fuel ratio control of S.I. engine has been conducted using modified sliding mode control methods. The experimental results show that the closed loop dynamics is much faster than that of the conventional sliding mode control. Transient air to fuel ratio excursion is considerably smaller than those of the production ECM. With the new control method, the time consuming gain tuning process can be avoided. The transient fueling compensation algorithm can be used with different types of engines and is insensitive to the aging of engine, since the technique identifies the engine characteristics on-line.

References

[1] Aquino, C.F., "Transient A/F Control Characteristics of the 5 Liter Central Fuel Injection Engine", SAE Paper No. 810494, 1981.

[2] Chang, C.-F., Fekete, N.P. and Powell, J.., "Engine Air-Fuel Ratio Using an Event-Based Observer", SAE Paper No. 930766, 1993. Theory", IEEE Trans. on Automatic Control, Vol. AC-25,No. 5, Oct. 1980.

[3] Cho, D. and Hedrick, J.K., "A Nonlinear Controller Design Method for Fuel-Injected Automotive Engines", ASME Trans. J. of Engine, Gas Turbines and Power, July 1988.

[4] Cho, D. and Hedrick, J.K., "Sliding Mode Fuel-Injection Controller: Its Advantages", ASME J. of Dynamic Systems, Measurement and Control, 113(3), pp537-541, Sep. 1991.

[5] Choi, S.-B. and Hedrick, J.K., "An Observer-based Controller Design Method for Automotive Fuel-Injection Systems",Proc. ACC, 1993, pp2567-2571.

[6] Falk, C.D. and Mooney, J.J., "Three-Way Conversion Catalysts: Effect of Closed-Loop Feed-Back Control and Other Parameters on Catalyst Efficiency", SAE Paper No.800462, 1980.

[7] Hendricks, E. and Sorenson, S.C., "SI Engine Controls and Mean Value Engine Modeling", SAE Paper No. 910258, 1991.

[8] Matthews, R.D. et. al., "Intake and ECM Submodel Improvements for Dynamic SI Engine Models: Examination of Tip-in/Tip-out", SAE Paper No. 910074, 1991.

[9] Sanner, R.M. and Slotine, J.J.E., "Gaussian Networks for Direct Adaptive Control", IEEE Transactions on Neural Networks Vol. 3, No. 6, 1992.

[10] Slotine, J.J.E. and Li, W., Applied Nonlinear Control, Prentice-Hall Inc., 1991.

[11] Utkin, V.I.(trans. by Parnakh, A.), Sliding Modes and Their Application in Variable Structure System, MIR Publishers, Moscow, 1978.